Originally published as:

Eva Eylert, Vroni Herrmann, Matthieu Jules, Nadine Gillmaier, Monika Lautner, Carmen Buchrieser, Wolfgang Eisenreich, and Klaus Heuner.
Isotopologue Profiling of *Legionella pneumophila*
Role of Serine and Glucose as Carbon Substrates
(2010) The Journal of Biological Chemistry, 285 (29), pp. 22232–22243.

DOI: 10.1074/jbc.M110.128678

Isotopologue Profiling of *Legionella pneumophila*

Role of Serine and Glucose as Carbon Substrates*

Eva Eylert[‡,1] Vroni Herrmann[§,1] Matthieu Jules[¶‖,2] Nadine Gillmaier[‡], Monika Lautner[§], Carmen Buchrieser[¶‖], Wolfgang Eisenreich[‡,3] and Klaus Heuner[§,4]

[‡]*Lehrstuhl für Biochemie, Technische Universität München, Lichtenbergstrasse 4, 85747 Garching, Germany*
[§]*Research Group P26-Nosocomial Infections of the Elderly, Robert Koch-Institut, Nordufer 20, 13353 Berlin, Germany*
[¶]*Institut Pasteur, Biologie des Bactéries Intracellulaires, F-75015 Paris, France*
[‖]*CNRS, URA 2171, F-75015 Paris, France*

Abstract

Legionella pneumophila (Lp) is commonly found in freshwater habitats but is also the causative agent of Legionnaires' disease when infecting humans. Although various virulence factors have been reported, little is known about the nutrition and the metabolism of the bacterium. Here, we report the application of isotopologue profiling for analyzing the metabolism of L. pneumophila. Cultures of Lp were supplied with [U-$^{13}C_3$]serine, [U-$^{13}C_6$]glucose, or [1,2-$^{13}C_2$]glucose. After growth, ^{13}C enrichments and isotopologue patterns of protein-derived amino acids and poly-3-hydroxybutyrate were determined by mass spectrometry and/or NMR spectroscopy. The labeling patterns detected in the experiment with [U-$^{13}C_3$]serine showed major carbon flux from serine to pyruvate and from pyruvate to acetyl-CoA, which serves as a precursor of poly-3-hydroxybutyrate or as a substrate of a complete citrate cycle with Si specificity of the citrate synthase. Minor carbon flux was observed between pyruvate and oxaloacetate/malate by carboxylation and decarboxylation, respectively. The apparent lack of label in Val, Ile, Leu, Pro, Phe, Met, Arg, and Tyr confirmed that L. pneumophila is auxotrophic for these amino acids. Experiments with [^{13}C]glucose showed that the carbohydrate is also used as a substrate to feed the central metabolism. The specific labeling patterns due to [1,2-$^{13}C_2$]glucose identified the Entner-Doudoroff pathway as the predominant route for glucose utilization. In line with these observations, a mutant lacking glucose-6-phosphate dehydrogenase (Δzwf) did not incorporate label from glucose at significant levels and was slowly outcompeted by the wild type strain in successive rounds of infection in Acanthamoeba castellanii, indicating the importance of this enzyme and of carbohydrate usage in general for the life cycle of Lp.

Abbreviations

Lp	*Legionella pneumophila*
PHB	poly-3-hydroxybutyrate
EMP	Embden-Meyerhof-Parnas
ED	Entner-Doudoroff
GC/MS	gas chromatography/mass spectrometry
PP	pentose phosphate
AYE	ACES-buffered yeast extract
ACES	2-[(2-amino-2-oxoethyl)amino]ethanesulfonic acid
BCYE	buffered charcoal-yeast extract
CDM	chemically defined medium
CFU	colony forming unit(s)
RT	reverse transcriptase
TBDMS	*tert*-butyldimethylsilyl
WT	wild type

Introduction

The Gram-negative bacterium *Legionella pneumophila* (*Lp*)[5] can be found in freshwater habitats where it replicates within protozoa, mainly amoebae such as *Acanthamoeba castellanii. Lp* can also be transmitted to humans by contaminated aerosols. After entering the human lung, the pathogen is phagocytosed by alveolar macrophages wherein it is able to replicate, leading to Legionnaires' disease, an atypical pneumonia.

Lp survives within amoebae and macrophages because of its ability to establish a replication vacuole that is derived from the endoplasmic reticulum. Once within a vacuole, *Lp* differentiates into the replicative form. When nutrients become limiting, a regulatory cascade triggers the differentiation to a spore-like mature intracellular form (MIF), the so-called transmissive form, which metabolically seems to be nearly dormant (1,–,6). These forms exhibit a thickened cell wall and high amounts of cytoplasmic granules of poly-3-hydroxybutyrate (PHB), a general energy and carbon storage compound of bacteria (1, 7, 8). When released from spent hosts, these transmissive forms of *Lp* are able to persist for long periods in the environment. It has also been shown that *Lp* is able to differentiate into a "viable but nonculturable" status of greatly reduced metabolic activity after persistence in water (9). Notably, *Legionella* species can also grow in defined culture media under laboratory conditions (10,–,15). However, less is known about the routes of nutrient utilization during growth in culture media as well as during intracellular multiplication (16,–,20).

Legionella exhibits a strictly respiratory form of metabolism and does not grow anaerobically (18). The amino acids Arg, Ile, Leu, Val, Met, Ser, and Thr are reportedly essential for growth of *Lp* in culture (10,–,12, 14, 15, 21,–,23), whereas a partial requirement for Cys (or cystine) has also been observed (24). It is also well known that *Lp* uses amino acids as preferred energy and carbon sources (4, 10,–,12, 14, 21, 22). More specifically, Ser, Glu, Tyr, and/or Thr are efficiently used as carbon and energy sources *in vitro* (14), and Cys, Gln, Ser, and Arg support growth *in vivo* (19). From *in silico* analysis of the known *Lp* genome sequences it is proposed that *Lp* is auxotrophic for the amino acids Cys, Met, Arg, Thr, Val, Ile, and Leu (18, 25, 26). Therefore, it is not surprising that *Lp* harbors genes for ~12 classes of ABC (ATP-binding cassette) transporters and amino acid permeases, as well as various different amino peptidases and proteases. In addition, it has been shown that amino acid transporters of the host cell and of *Lp* are essential for intracellular replication; specifically, a neutral amino acid transporter of the host cell (SLC1A5 of MM6 monocyte cells) is necessary for *Lp* to replicate within this host (19). Furthermore, a bacterial Thr transporter (PhtA) is reported to be essential for replication of *Lp* in bone marrow-derived macrophages from mice (27).

In earlier studies, it was also suggested that *Lp* is able to use glucose as a carbon source (14, 15, 20), although the addition of glucose to the medium did not support *in vitro* growth (18, 20). As no active sugar transport could be demonstrated *in vitro* (14, 16, 18), it is generally believed that *Lp* does not utilize sugars as a carbon source but relies on gluconeogenesis (18). On the other hand, some of the various ABC-type transport systems might be involved in sugar uptake, because *Lp* also possesses putative systems for degradation of cellulose, chitin, starch, and glycogen (28). Recently, *Lp* has been shown to actively degrade cellulose (29). On the basis of this evidence it can be assumed that glucose is also catabolized, but the metabolic routes are still unknown.

The four sequenced genomes of *Lp* (*Lp* Philadelphia (26), *Lp* Paris, *Lp* Lens (25), and *Lp* Corby (30) indicate the presence of the Embden-Meyerhof-Parnas (EMP) pathway as well as the Entner-Doudoroff (ED) pathway. However, *in vitro* enzyme assays did not detect activities for the ED pathway in strains Knoxville-1 and Philadelphia-1 (17, 20). Genes encoding the pentose phosphate (PP) pathway are also present, with the exception of 6-phosphogluconate dehydrogenase and the transaldolase (16, 18, 25, 26).

As the activity of pyruvate dehydrogenase was low in cell-free extracts (17, 20), it was hypothesized that the bulk of the acetyl-CoA entering the citrate cycle or used as precursor for the storage compound PHB is derived from fatty acid catabolism (18). Indeed, *Lp* possesses huge amounts of phospholipases exerting extracellular and cell-associated activities (31,–,33). However, the glyoxylate shunt appears to be absent in the *Lp* strains sequenced thus far.

One powerful method of studying metabolic pathways in growing microbes is based on incorporation experiments with stable isotope-labeled precursors (*e.g.* ^{13}C-labeled glucose) followed by the determination of the resulting isotopologue patterns in key metabolites, such as protein-derived amino acids or other storage compounds. Using stoichiometric models, isotopologue profiles can serve as constraints in metabolic flux calculations (^{13}C-based metabolic flux analysis) (34). Metabolic flux analysis is now well established for the analysis of metabolic flux in microorganisms growing under standardized conditions (reviewed in Refs. 34 and 35). These models typically rely on the use of minimal media with only one possible carbon source. It is therefore difficult to adapt metabolic flux analysis calculations to organisms with complex multiple carbon usage (*i.e.* when growing in complex media). However, because of the specificity of the detected isotopologue profiles, observation-driven analysis can also trace metabolic pathways in cases with unknown and/or multiple carbon usage (36, 37). In this study, the metabolism of *Lp* grown under culture conditions was analyzed for the first time by ^{13}C-labeled isotopologue (^{13}C-isotopologue) profiling using glucose or Ser as precursors.

Experimental Procedures

Strains, Growth Conditions, and Media

A. castellanii ATCC30010 was cultured in PYG 712 medium (2% proteose-peptone, 0.1% yeast extract, 0.1 m glucose, 4 mm $MgSO_4$, 0.4 m $CaCl_2$, 0.1% sodium citrate dihydrate, 0.05 mm $Fe(NH_4)_2(SO_4)_2 \times 6\ H_2O$, 2.5 mm NaH_2PO_4, and 2.5 mm K_2HPO_4) at 20 °C. *Escherichia coli* DH5α was used to clone recombinant plasmid DNA. Experiments were done with *L. pneumophila* Paris (CIP 107629 (25)). As described previously (28), *Lp* strains were cultured in AYE medium (ACES-buffered yeast extract broth: 10 g of ACES, 10 g of yeast extract, 0.4 g of l-cysteine, and 0.25 g of iron pyrophosphate in 1 liter (pH 6.8)) (see also supplemental Table S1) or on ACES-buffered charcoal-yeast extract (BCYE) agar plates at 37 °C. Alternatively, *Lp* Paris was cultivated in a chemically defined medium (CDM) (for details see supplemental Table 1) adapted from Ristroph *et al.* (12).

^{13}C Labeling Experiments

1 liter of growth medium (AYE or CDM) was supplemented with 2 g of [U-$^{13}C_6$]glucose, 2 g of [1,2-$^{13}C_2$]glucose, or 0.3 g of [U-$^{13}C_3$]Ser. 500 ml of the supplemented AYE medium was inoculated with 1 ml of an overnight culture of *Lp* Paris. For supplemented CDM the inoculum was 4 ml of an overnight culture grown in AYE medium. Incubation was carried out at 37 °C and 220 rpm, and the optical density at 600 nm (A_{600}) was determined at regular intervals. An A_{600} of 1.0 was determined as exponential growth, whereas an A_{600} of ~2.0 correlated with stationary growth. Cultures in AYE medium reached exponential growth after 16 h and stationary growth at 29 h. Cultures grown in CDM became stationary at 40 h. Before harvesting, a culture aliquot was plated on LB agar plates to rule out the possibility of contamination. The bacteria were killed with sodium azide at a final concentration of 10 mm and pelleted at 5500 × *g* and 4 °C for 15 min. The pellet was washed twice with 200 ml of water and then once with 2 ml of water. The supernatant was discarded, and the bacterial pellet was autoclaved at 120 °C for 20 min.

Strain Construction

The *lpp0483* mutant strain of *Lp* Paris (Δ*zwf*) was constructed as described previously (28, 38). In brief, the gene *lpp0483* (*zwf*) was inactivated by insertion of a kanamycin resistance (kan^R) cassette into the chromosomal gene. The chromosomal region containing the *lpp0483* gene was PCR-amplified with the primers lpp0483_for and lpp0483_rev, and the product (2639 bp) was cloned into the pGEM-T Easy vector (Promega). On this template, an inverse PCR was performed using the primers lpp0483_inv_for and lpp0483_inv_BamHI_rev, with the reverse primer bearing a BamHI restriction site. These primers amplified 4912 bp corresponding to the pGEM backbone and the flanking regions of *lpp0483*. The resulting PCR product was BamHI-digested and ligated to the kan^R cassette (1210 bp amplified via PCR from the plasmid pGEM-Kan^R subcloned into a pGEM-T Easy vector) using primers containing BamHI restriction sites at the ends (Kan_BamHI_for and Kan_BamHI_rev). All primers are listed in Table 1. For chromosomal recombination, the construct (*i.e.* PCR fragment containing the kan^R cassette with flanking regions of the gene of interest, ~900 bp upstream and ~250 bp downstream) was introduced into the *Lp* Paris strain by transformation. Three independent Δ*zwf* mutant strains were generated, and two of them were used for intracellular replication assays.

Intracellular Multiplication in A. castellanii

For *in vivo* growth of *Lp* Paris and its derivatives in *A. castellanii*, we followed a protocol described previously (28). In brief, 3-day-old cultures of *A. castellanii* were washed in AC buffer (PYG 712 medium without proteose-peptone, glucose, and yeast extract) and adjusted to 5 × 10^5 cells. Stationary phase *Legionella* bacteria grown on BCYE agar were diluted in water and mixed with *A. castellanii* at a multiplicity of infection of 0.01. After invasion for 1 h at 37 °C, the *A. castellanii* layer was washed twice, defining the start point of the time course experiment. The number of colony forming units (CFU) of legionellae was determined by plating on BCYE agar. Each infection was carried out in duplicates and was done at least three times.

Intracelluar Multiplication/Survival in A. castellanii

The intracellular multiplication was carried out as described above but without the washing step. After 3 days, *A. castellanii* cells were resuspended, 100-µl aliquots were lysed, and serial dilutions were spread on BCYE agar to determine the number of CFU. To study the replication rates in repeating rounds of infection, the remaining solution was incubated at 37 °C for a further 3 days and diluted (1:1000). The number of CFU was determined by plating the remaining solution on BCYE agar. 1 ml of the remaining dilution was used to reinfect fresh amoeba cultures as described previously. Four rounds of infection were performed in total, and each infection was carried out in duplicates and done at least three times.

Intracelluar Multiplication/Survival Assay in "Competition"

The infection procedure was similar to the assay described above, but equal amounts of bacteria of the wild type and the Δ*zwf* mutant strain (kanamycin resistant) were used together to co-infect the *A. castellanii* cells. After 3 days, *A. castellanii* cells were resuspended, 100-µl aliquots were lysed, and serial dilutions were spread on BCYE agar with and without kanamycin to determine the number of CFU. The remaining infection solution was incubated at 37 °C for a further 3 days and diluted (1:1000). The resulting solution was used to determine the number of CFU on BCYE with and without kanamycin and to reinfect fresh amoebae. Four rounds of infection were performed in total. To determine the number of wild type bacteria, the CFU on BCYE-kanamycin agar was subtracted from the CFU on BCYE plates without kanamycin. In the survival assay, the mixture of the first infection was incubated for a further 19 days. To follow the Δ*zwf* and WT strain recovery capabilities, each sample was plated (100 µl) on BCYE and/or BCYE-kanamycin plates. Each infection was carried out in duplicates and was done at least three times.

RT-PCR

Total RNA was extracted from bacteria grown in AYE medium to the appropriate growth phase, incubated with Dnase I, and then repurified. RT-PCR reactions were performed with a OneStep RT-PCR kit (Qiagen) using gene-specific primers. The RT reaction was carried out at 50 °C for 30 min with 0.5 µg of total RNA. PCR amplification was performed with each primer at 0.6 µm and each dNTP at 400 µm in 1× OneStep RT-PCR buffer containing 12.5 mm $MgCl_2$ and 2 µl of OneStep RT-PCR enzyme mix. The total volume was 50 µl. The cycling conditions were 94 °C for 1 min, 53–55 °C for 1 min, and 72 °C for 1 min for 25 to 35 cycles with a Thermocycler. The following gene-specific primer pairs were used: accC-For and accC-Rev; edd-For and edd-Rev; fadD-For and fadD-Rev; fumC-For and fumC-Rev; pfp-For and pfp-Rev; pykA-For and pykA-Rev; ppsA-For and ppsA-Rev; rpiA-For and rpiA-Rev; and sucA-For and sucA-Rev. All primers used for RT-PCR are listed in Table 1.

Primers used in this study

Protein Hydrolysis and Amino Acid Derivatization

Bacterial cell mass was suspended in 6 m hydrochloric acid and heated at 105 °C for 24 h under an inert atmosphere. The hydrolysate was placed on a cation exchange column of Dowex 50W×8 (H^+ form, 200–400 mesh, 5 × 10 mm) that was washed with water and developed with 2 m ammonium hydroxide. An aliquot of the eluate was dried under a stream of nitrogen, and the residue was dissolved in 50 µl of water-free acetonitrile. A mixture of 50 µl of *N*-(*tert*-butyldimethylsilyl)-*N*-methyl-trifluoroacetamide containing 1% *tert*-butyldimethylsilylchloride (Sigma) was added. The mixture was kept at 70 °C for 30 min. The resulting *N*-(*tert*-butyldimethylsilyl) (TBDMS)-amino acids were then analyzed by GC/MS.

Dichloromethane Extraction and Isolation of Amino Acids

The dried sample was heated under reflux with 10 ml of dichloromethane/100 mg of sample for 1 h. After filtration the filtrate was evaporated.

The filtered residue was dried and hydrolyzed with 6 m hydrochloric acid containing 0.5 mm thioglycolic acid. The mixture was boiled for 24 h under an inert atmosphere and then filtered. The solution was concentrated to a small volume under reduced pressure and lyophilized. The residue was dissolved in 8 ml of water. The solution was placed on top of a column of Dowex 50W×8 (H^+ form, 3 × 33 cm). The column was washed with 300 ml of water and then was developed with a linear gradient of 0–3 m hydrochloric acid (total volume, 2 liters). Fractions were collected, combined, evaporated to a small volume under reduced pressure, and lyophilized (36).

Mass Spectrometry

GC/MS analysis was performed on a GC-17A gas chromatograph and/or GC 2010 (Shimadzu, Duisburg, Germany) equipped with a fused silica capillary column (Equity TM-5; 30 m × 0.25 mm, 0.25 μm film thickness; SUPELCO, Bellefonte, PA) and a QP-5000 and/or GC-QP2010 plus mass selective detector (Shimadzu) working with electron impact ionization at 70 eV. An aliquot (1 μl) of a solution containing TBDMS amino acids was injected in a 1:10 split mode at an interface temperature of 260 °C and a helium inlet pressure of 70 kilopascals. The column was developed at 150 °C for 3 min and then with a temperature gradient of 10 °C/min to a final temperature of 280 °C that was held for 3 min. Data were collected using Class 5000 and/or GCMS Solution software (Shimadzu). Selected ion monitoring data were acquired using a 0.3-s sampling rate. Samples were analyzed at least three times. The theoretical isotope ratio and numerical deconvolution of the data were computed according to standard procedures: (i) determination of the "TBDMS derivate" spectrum of TBDMS-amino acid, (ii) determination of the mass isotopomer distribution of the labeled amino acid, and (iii) correction for incorporation of ^{13}C from natural abundance into that amino acid (39).

NMR Spectroscopy

^{1}H and ^{13}C NMR spectra were recorded at 25 °C using a DRX-500 spectrometer (Bruker Instruments, Karlsruhe, Germany) at transmitter frequencies of 500.1 and 125.6 MHz, respectively. Extracts with dichloromethane were dissolved in $CDCl_3$, and amino acids were measured in 0.1 m DCl. ^{13}C enrichments were determined by quantitative NMR spectroscopy. For this purpose, ^{13}C NMR spectra of the biolabeled specimens and of samples with natural ^{13}C abundance (*i.e.* with 1.1% ^{13}C abundance) were measured under the same experimental conditions. The ratios of the signal integrals of the labeled compounds and of the compounds at natural abundance were then calculated for each respective carbon atom. Absolute ^{13}C abundances for certain carbon atoms (*i.e.* for carbon atoms with at least one attached hydrogen atom displaying a ^{1}H NMR signal in an uncrowded region of the spectrum) were determined from the ^{13}C coupling satellites in the ^{1}H NMR spectra. The relative ^{13}C abundances determined for all other positions were then referenced to this value, thus affording absolute ^{13}C abundances for every single carbon atom. ^{13}C-coupled satellites were integrated separately. The relative fractions of each respective satellite pair (corresponding to a given coupling pattern) in the total signal integral of a given carbon atom were calculated. These values were then referenced to the global ^{13}C abundance affording concentrations of multiple ^{13}C-labeled isotopologue groups (mol %).

Results

Growth of Lp in Culture under Standardized Conditions

Cultures of *Lp* can be grown in various media although not in a medium that comprises only one possible carbon source. Typically, so-called AYE medium is used, which consists of yeast extract and ACES buffer and high amounts of iron ions and cysteine. However, it is also possible to use a chemically defined medium consisting of ACES, 16 amino acids (not included are Ala, Gly, Asn, and Gln), ammonium chloride, and some inorganic salts (again including high amounts of iron ions; for details, see supplemental Table S1). To estimate the impact of the culture medium on the growth and metabolism of *Lp*, we cultivated the bacterium for 2 days at 37 °C in duplicates in 500 ml of AYE medium or CDM, each supplemented with 11 mm glucose. At timed intervals, the optical density at 600 nm (A_{600}) and the CFU were determined. *Lp* Paris had a generation time of 2.7 h in AYE medium and 4.4 h in CDM, and the final cell densities (optical density) were ~2.1 and 1.4, respectively (data not shown).

Serine Serves as a Major Carbon Substrate for Lp

In earlier studies, Ser was shown to support the growth of *Lp* (10, 14, 15), and high activity levels of Ser dehydratase converting Ser into pyruvate were detected in cell-free extracts of the bacterium (20).

To analyze the metabolic fate of Ser in more detail, we added 3 mm [U-$^{13}C_3$]Ser to the AYE medium (for details, see "Experimental Procedures") and grew *Lp* for 29 h until the cells entered stationary phase (*A* = 2.1 at 600 nm). PHB and amino acids were extracted from the cells and analyzed by GC/MS and/or quantitative NMR spectrometry (for details, see "Experimental Procedures").

NMR Analysis of the Dichloromethane Extract

The ^{13}C NMR spectrum of the dichloromethane extract showed four intense signals due to PHB (supplemental Fig. S1*A*; Table 2). Notably, the spectrum did not display signals of lipids or fatty acids at significant concentrations. All PHB signals showed pairs of satellites due to $^{13}C^{13}C$ couplings at high intensities. The quantitative signal analysis (Table 3) showed that ~3 mol % of PHB was multiply ^{13}C-labeled and therefore derived from the supplied [U-$^{13}C_3$]Ser or a multiply ^{13}C-labeled downstream product. The coupling pattern (*i.e.* the size of the coupling constants for each carbon signal; Table 2) clearly showed that [1,2-$^{13}C_2$]- and [3,4-$^{13}C_2$]PHB were the predominant multiply ^{13}C-labeled species. The isotopologue pattern can be explained by the well known mechanisms of PHB formation (7, 8) from [1,2-$^{13}C_2$]acetyl-CoA and unlabeled acetyl-CoA (from the degradation of unlabeled components present in AYE medium) affording [1,2-$^{13}C_2$]acetoacetyl-CoA or [3,4-$^{13}C_2$]acetoacetyl-CoA (Fig. 1). Reduction yielded 3-[1,2-$^{13}C_2$]- or 3-[3,4-$^{13}C_2$]hydroxybutyryl-CoA, respectively, which was then condensed to PHB with the detected isotopologue composition. The minor U-$^{13}C_4$-isotopologue in PHB can be explained by the statistical combination of two molecules of [1,2-$^{13}C_2$]acetyl-CoA.

GC/MS Analysis of Protein-derived Amino Acids

GC/MS analysis showed that 25% of the protein-derived Ser carried ^{13}C label (Fig. 2, *gray bar*; see numerical values in supplemental Table S3). Not unexpectedly, this finding documented that exogenous Ser was efficiently incorporated into *Lp* and was used for protein biosynthesis. The high ^{13}C enrichment values of other amino acids (3–12%; Ala > Glu > Gly = Asp; Fig. 2, *gray bars*) as well as the ^{13}C enrichment in PHB (3%) indicated that Ser was also shuffled into the central carbon metabolism of *Lp* where it was converted into pyruvate/Ala, oxaloacetate/Asp, and α-ketoglutarate/Glu, as well as into acetyl-CoA serving as a precursor of PHB. However, the ^{13}C enrichments of those metabolites were significantly lower (3–12%) than that of Ser (25%) suggesting (i) that higher fractions of Ala, Glu, Gly, and Asp were incorporated from the medium (*i.e.* in unlabeled form) as compared with Ser; and/or (ii) as expected, that Ser was not the unique carbon source for *Lp* under the experimental conditions and that, next to ^{13}C-labeled Ser, unlabeled carbon substrates were shuffled into the biosynthetic pathways of Ala, Glu, Gly, and Asp. The lack of label in Ile, Leu, Val, and Tyr showed that these amino acids were derived from unlabeled amino acids present in the medium and/or were not synthesized *de novo*. Albeit with high standard deviations, a slight ^{13}C enrichment was detected in Pro, Thr, and Tyr. It remains open as to whether these amino acid were made *de novo* under the experimental conditions (16, 18).

The mass data also revealed the abundances of ^{13}C-labeled isotopologues comprising a given number of ^{13}C atoms (Fig. 2, *patterned columns*; see numerical values in supplemental Table S4). Ser and Ala were characterized by $^{13}C_3$-isotopologues, whereas Asp and Glu were more complex mixtures of species comprising one, two, and three ^{13}C-labeled atoms (Fig. 2). Gly was a mixture of $^{13}C_1$- and $^{13}C_2$-isotopologues.

NMR Analysis of Protein-derived Amino Acids

To localize the label distribution at higher resolution, purified amino acids were also analyzed by quantitative NMR spectroscopy (36). Many of the ^{13}C NMR signals were multiplets caused by couplings between adjacent ^{13}C atoms in a given molecule. As examples, ^{13}C NMR signals of the C-3 of Asp and the C-2 of Ala are shown in supplemental Fig. S2. From the signal intensities of the satellites, the molar abundances of the underlying isotopologues were calculated and referenced to the values obtained by mass spectrometry. The coupling patterns of all labeled amino acids are shown graphically in Fig. 3 with *bars* connecting ^{13}C-labeled atoms in multiple ^{13}C-labeled isotopologues (see also supplemental Table S5).

The labeling patterns of Ser and Ala were characterized by a high abundance of the triple ^{13}C-labeled isotopologues and minor amounts of 1,2-$^{13}C_2$-isotopologues. The triple ^{13}C-labeled isotopologues of Ser and Ala can be explained easily by the direct incorporation of exogenous [U-$^{13}C_3$]Ser into the protein-derived Ser and Ala fractions, respectively. The metabolic precursor for [U-$^{13}C_3$]Ala is [U-$^{13}C_3$]pyruvate. It appears safe to assume that the later compound is derived from [U-$^{13}C_3$]Ser by Ser dehydratase (Fig. 3, *red arrow*). The detection of the 1,2-$^{13}C_2$-isotopologues lends support for the existence of Ser recycling via reactions of gluconeogenesis (Fig. 3). More specifically, the formation of phosphoenolpyruvate from [1,2-$^{13}C_2$]oxaloacetate (Fig. 3, *green arrow*) was conducive to the formation of [1,2-$^{13}C_2$]phosphoenolpyruvate and 3-[1,2-$^{13}C_2$]phosphoglycerate serving as the precursor of [1,2-$^{13}C_2$]Ser, which was then further converted into [1,2-$^{13}C_2$]pyruvate/Ala by Ser dehydratase.

The labeling profile of PHB can be taken as a reference for the labeling pattern of its precursor, acetyl-CoA. On this basis, the presence of [1,2-$^{13}C_2$]acetyl-CoA reflected its formation from [U-$^{13}C_3$]- and [1,2-$^{13}C_2$]pyruvate by pyruvate dehydrogenase. This isotopologue was then used for PHB synthesis but could also be shuffled into the citrate cycle, affording specific isotopologue profiles in α-ketoglutarate and oxaloacetate, which serve as precursors for Glu and Asp, respectively (Fig. 3). Because of a *Si*-specific citrate synthase, label from [1,2-$^{13}C_2$]acetyl-CoA (Fig. 3, *red bar*) was transferred to positions 4 and 5 of α-ketoglutarate and glutamate. Following the reactions of the citrate cycle, label from α-[4,5-$^{13}C_2$]ketoglutarate afforded [1,2-$^{13}C_2$]succinate and [1,2-$^{13}C_2$]fumarate (Fig. 3, *red bars*). Because of the intrinsic symmetry of fumarate, malate synthase yielded a 0.5:0.5 mixture of [1,2-$^{13}C_2$]- and [3,4-$^{13}C_2$]malate from [1,2-$^{13}C_2$] fumarate. (Fig. 3, *green bars*). The same isotopologue mixture resulted in oxaloacetate and its amination product, aspartate (Fig. 3, *green bars* and M+2 values from the mass spectrum). The presence of triple ^{13}C-labeled isotopologues in Asp (Fig. 3, *blue bars* and M+3 values) also reflected the formation of oxaloacetate by carboxylation of [U-$^{13}C_3$]pyruvate (Fig. 3, *blue arrow*). Primarily, this reaction yielded from [U-$^{13}C_3$]pyruvate [1,2,3-$^{13}C_3$]oxaloacetate, which was then converted into [1,2,3-$^{13}C_3$]Asp. The fact that [2,3,4-$^{13}C_3$]oxaloacetate/Asp also was observed at similar abundances as found for the 1,2,3-$^{13}C_3$-isotopologue can be explained by rapid equilibrium between oxaloacetate/malate/fumarate due to reversible malate dehydrogenase, malate synthase, and possibly also succinate dehydrogenase. Because of the symmetry of fumarate and succinate, the triple label was then randomized, affording the observed symmetric isotopologue distribution in oxaloacetate/Asp.

Labeled oxaloacetate also served as an acceptor of unlabeled acetyl-CoA. As shown in Fig. 3, label from [3,4-$^{13}C_2$]oxaloacetate was transferred to positions 1 and 2 of α-ketoglutarate/Glu (*green bar*), and [1,2-$^{13}C_2$]oxaloacetate yielded [3-$^{13}C_1$]Glu. Label from position 1 of oxaloacetate was lost as $^{13}CO_2$ during dehydrogenation of isocitrate. [1,2,3-$^{13}C_3$]- and [2,3,4-$^{13}C_3$]oxaloacetate gave rise to 2,3-$^{13}C_2$- and 1,2,3-$^{13}C_3$-labeled species in α-ketoglutarate/Glu, respectively. Notably, all of these isotopologues were detected in glutamate, although [1,2,3-$^{13}C_3$]Glu could be identified only by mass spectrometry (as M+3 species).

Lp Is Able to Use Glucose as a Carbon Source

To obtain information about a potential usage of glucose, *Lp* was grown in AYE medium or CDM supplemented with 11 mm [U-$^{13}C_6$]glucose and harvested at stationary phase. A sample work-up and analysis were done as described above. Fig. 4 indicates that the same set of amino acids labeled from [^{13}C]Ser also acquired significant ^{13}C label (>1% ^{13}C enrichment; Ala > Glu > Asp > Pro > Ser) from [U-$^{13}C_6$]glucose supplemented either to the AYE medium or to CDM. The percentage of enrichment values of amino acids was remarkably similar, pointing to glucose metabolism irrespective of the culture medium used. In contrast to the small differences in the ^{13}C enrichments of amino acids, we noticed a rather large difference in the ^{13}C incorporation of [U-$^{13}C_6$]glucose into PHB. More specifically, ^{13}C enrichment of PHB isolated from cells grown in AYE medium was ~3-fold higher than the corresponding value in the experiments using CDM. The labeling patterns from the experiment with AYE medium are discussed in detail below.

Elevated Rate of Glucose Incorporation into PHB

The ^{13}C NMR signals of PHB detected in the dichloromethane extract of the labeled cells (supplemental Fig. S1*B*) displayed the same coupling pattern as observed previously for PHB labeled from [U-$^{13}C_3$]Ser. However, the intensities of the coupling satellites relative to the central signals were

higher in the experiment with [U-$^{13}C_6$]glucose (Table 3). The analysis of the signals corroborated the fact that [1,2-$^{13}C_2$]- and [3,4-$^{13}C_2$]PHB were again the dominant species, each with abundances of approximately 5%. As described above in detail, this isotopologue mixture can be explained by PHB biosynthesis from a mixture of 1,2-$^{13}C_2$-labeled and unlabeled acetyl-CoA. The minor [U-$^{13}C_4$]PHB species was again assembled from two labeled molecules of acetyl-CoA. In summary, these data demonstrated that [U-$^{13}C_2$]acetyl-CoA can be made from [U-$^{13}C_3$]Ser or [U-$^{13}C_6$]glucose, indicating that Ser and glucose catabolism merge at a certain stage of the intermediary metabolism (*i.e.* prior to acetyl-CoA formation). During growth in AYE medium, glucose appeared to be used preferably as a PHB precursor. Under these conditions more than 6 mol % of PHB was derived from exogenous [^{13}C]glucose (as compared with 0–5 mol % in amino acids).

Amino Acids

The ^{13}C incorporation into the bacterial amino acids as determined by GC/MS and NMR was 0.5–5% in the following order: Ala > Asp > Glu > Ser > Gly (Figs. 4 and 5). The same set of amino acids was also found to be labeled from [U-$^{13}C_3$]Ser, although at higher rates (3–12%). Generally, the relatively low incorporation rates of glucose into amino acids suggested that glucose did not serve as a major carbon source during the overall growth period of the experiment. Notably, the incorporation of glucose into pyruvate/alanine (4.9%) was considerably lower than the rate into PHB (6.3%). This was in sharp contrast to the values of the experiment with [U-$^{13}C_3$]Ser where the incorporation rate into PHB was lower (3.2%) than the respective value into pyruvate/alanine (12.2%). The discrepancy between the ^{13}C enrichments in pyruvate (serving as precursor for Ala) and acetyl-CoA (serving as precursor for PHB) immediately showed that these intermediates were not in isotopic equilibrium.

Ile, Leu, Phe, Tyr, His, Pro, and Val were also found to be unlabeled from [U-$^{13}C_6$]glucose. This confirms that *Lp* is auxotrophic for these amino acids as suggested. Surprisingly, some label appeared to be transferred from glucose to Ser, although exogenous Ser had been shown to be incorporated efficiently into proteins in the previous experiment. Moreover, a weak ^{13}C enrichment of Thr also could not be excluded on the basis of our experimental data.

The isotopologue distribution in each of the labeled amino acids was then determined by mass spectrometry and NMR spectroscopy as described before. Ala was characterized by the U-$^{13}C_3$-isotopologue. This isotopologue can be explained by glucose utilization via glycolysis, the PP pathway, and/or the ED pathway (Fig. 6). At lower abundances, Ser was also present as a U-$^{13}C_3$-isotopologue, suggesting that 3-phosphoglycerate acquired at least some ^{13}C label by glycolysis. [1,2-$^{13}C_2$]Ala was observed as a minor isotopologue, suggesting that a small fraction of phosphoenolpyruvate/ pyruvate was made from [1,2-$^{13}C_2$]oxaloacetate by decarboxylation (Fig. 6, *green arrow*). The labeling patterns in Asp and Glu supported carbon flux via the complete citrate cycle as already shown by the respective labeling profiles from [U-$^{13}C_3$]Ser. Thus, formation of oxaloacetate from pyruvate was again detected on the basis of $^{13}C_3$-isotopologues in Asp and 1,2,3-$^{13}C_3$- and 2,3-$^{13}C_2$-isotopologues in Glu.

Glucose Is Catabolized by the Entner-Doudoroff Pathway in Lp

To determine the glucose utilization pathway, we performed a labeling experiment with *Lp* Paris (*Lp*) in AYE medium supplemented with 11 mm [1,2-$^{13}C_2$]glucose. The ^{13}C enrichments and patterns in amino acids and PHB (Fig. 4, *lane e*) followed the same rules as described above. As shown in supplemental Fig. S3, label from [1,2-$^{13}C_2$]glucose was transferred at high rates to [1,2-$^{13}C_2$]Ala via the ED pathway but not to a 2,3-$^{13}C_2$-labeled specimen representing a hypothetical product via glycolysis. Moreover, the apparent lack of label in Ser was also in line with the ED pathway, because glycolysis should have generated [2,3-$^{13}C_2$]Ser. The PP pathway was also excluded as a major pathway for utilizing glucose because no or only single labeled pyruvate/Ala (^{13}C at C-3) should have occurred when [1,2-$^{13}C_2$]glucose was catabolized by this route. The low, single ^{13}C enrichment at C-1 of pyruvate/Ala rather reflected minor carbon flow from [^{13}C]oxaloacetate as already outlined above (supplemental Fig. S3). Pyruvate dehydrogenase should yield [1-$^{13}C_1$]acetyl-CoA from [1,2-$^{13}C_2$]pyruvate. [1-$^{13}C_1$]Acetyl-CoA was then conducive to the detected [1-$^{13}C_1$]- and [4-$^{13}C_1$]PHB specimens. The labeling patterns of Asp and Glu were also in full accordance with the carbon fluxes described above for the earlier

experiments. Thus, our results identified the ED pathway as the predominant route of glucose catabolism in *Lp*.

Construction, Properties, and Isotopologue Profiling of a Δzwf Mutant Strain

To further investigate the role of the ED pathway for glucose utilization in *Lp*, we constructed a mutant of *Lp* Paris in which we deleted the gene *lpp0483* (Δ*zwf*), which codes a key enzyme of the ED pathway necessary for the conversion of glucose 6-phosphate into 6-phosphogluconolactone (Fig. 7). To investigate whether the putative *zwf* operon (*lpp0483–0488*) is expressed as a polycistronic mRNA, we conducted RT-PCR experiments. Indeed, the genes *lpp0483* to *lpp0487* were co-transcribed; however, gene *lpp0488* encoding a putative glucose transporter was transcribed separately (Fig. 7). To exclude possible downstream effects of the deletion of *zwf*, we analyzed the transcription of the downstream genes, which confirmed that there were no polar effects due to the mutation (data not shown).

The Δ*zwf* mutant was then grown in AYE medium containing [U-$^{13}C_6$]- or [1,2-$^{13}C_2$]glucose as described above for the wild type strain. The Δ*zwf* mutant strain showed strongly reduced incorporation rates (by an approximate factor of 10) into PHB and amino acids (Fig. 4, *lanes f* and *g*). On the basis of this drastic modulation, we concluded (i) that the protein encoded by *lpp0483* was functionally involved in glucose metabolism and most probably catalyzed the presumed conversion of glucose 6-phosphate into 6-phosphogluconolactone and (ii) that the ED pathway was the predominant route for glucose catabolism. Nevertheless, the occurrence of ^{13}C label in Ala and PHB (clearly indicated by the mass spectrum of alanine and the coupling satellites in the NMR spectrum of alanine and PHB; *cf*. supplemental Fig. S1 and Table 3) showed that [U-$^{13}C_6$]glucose was still converted (albeit at very low rates) into pyruvate and acetyl-CoA serving as precursors for alanine and PHB, respectively. It can be hypothesized that the minor flux of glucose into pyruvate and acetyl-CoA existed via glycolysis in the mutant. Notably, the enzymes required for glycolytic conversion of glucose are present in the genome of *Lp*.

Hints for a Functional Role of Carbohydrate Utilization by Lp

To better understand the role of glucose metabolism in the life cycle of *Lp*, we ran infections of *A. castellanii*. The deletion of *zwf* in *Lp* did not significantly affect replication within the host (Fig. 8*A*). However, this was different when replication during successive rounds of infection was analyzed. After a first infection, which lasted 3 days, the mixture (comprising amoeba lysate and *Lp* WT or Δ*zwf* mutant strain) was kept for 3 additional days. Then, we ran another infection using 1 ml of a 1:1000 dilution of the previous mixture in fresh infection buffer with fresh amoebae. To follow infection kinetics, each sample was plated on BCYE and/or BCYE kanamycin plates. Although there was only a minor difference during the second and third round of infection of amoebae (Fig. 8*B*), we noted that the viability of the Δ*zwf* mutant strain dropped during the lag period. We then verified this observation by an experiment with a lag period of 20 days between the first and second rounds of co-infection and by evaluating the recovery percentage (ratios of Δ*zwf*/Δ*zwf* + WT) of both the mutant and the wild type strain (Fig. 8*C*). Then, we performed competition experiments with successive rounds of infection using the Δ*zwf* mutant strain and the WT strain. Again, the mutant strain showed less fitness, and the observed effect accumulated with each additional round of infection until the mutant strain was outcompeted by the WT strain (Fig. 8*D*). Altogether, these results indicate an important role of the ED pathway (glucose-6-phosphate dehydrogenase) for the survival of *Lp* in the environment.

Discussion

Lp survives within amoebae and macrophages because of its ability to establish a replication vacuole that is derived from the endoplasmic reticulum. Within this vacuole, *Lp* differentiates into the replicative form and multiplies. It was proposed that when nutrients become limiting, a regulatory cascade triggers the differentiation to a motile spore-like form. After the bacteria are released from the host cells, these forms of *Lp* are well prepared to persist for long periods in the environment. It is known that *Legionella* exhibits a strictly respiratory form of metabolism and does not grow anaerobically (18). It is also current knowledge that *Lp* uses amino acids as primary energy and carbon sources (4, 10,–,12, 14) and that metabolic genes are expressed mainly in the exponential growth phase during *in vivo* growth within *A. castellanii* (28).

In this study, the metabolism of *Lp* was analyzed for the first time by comprehensive isotopologue profiling under culture conditions. Metabolic fluxes were estimated on the basis of the observed labeling profiles in amino acids and PHB. It had been reported previously that Ser is actively metabolized by legionellae and that Ser is necessary for the growth of *Lp* (10, 12, 14,–,16, 18, 19, 27). In the genome of strain Paris genes encoding for ~12 ABC transporters and amino acid permeases, *e.g.* a putative Ser transport protein (Lpp2269) and the putative amino acid transporters Lpp0026 and Lpp0357 are predicted. Indeed, using [U-$^{13}C_3$]Ser as a supplement to AYE medium at a concentration of 3 mm, label was transferred to protein-derived [$^{13}C_3$]Ser at ~25%. Assuming that yeast extract present in AYE medium contributes unlabeled Ser at a similar concentration as the added ^{13}C-labeled Ser (see also supplemental Table S1), the incorporation of exogenous Ser into protein-derived Ser can be estimated as 50%. This high value supports the view that amino acid transporters, accepting Ser as a substrate, are active in *Lp*. Albeit at lower levels of ^{13}C enrichment (0–13%), label from [U-$^{13}C_3$]Ser was also distributed to other amino acids (Ala, Glu, Gly, and Asp) as well as to PHB. This lends evidence that Ser is catabolized to pyruvate by Ser dehydratase, known to be active in cell extracts of *Lp* (20). The enrichment values and isotopologue profiles of the storage compound, PHB, and amino acids derived from intermediates of the citrate cycle (*i.e.* Asp and Glu) also demonstrate that a carbon flux exists from pyruvate to acetyl-CoA serving as a precursor of PHB and a substrate of a complete citrate cycle with *Si* specificity of citrate synthase. Our data did not show any evidence for a functional glyoxylate bypass, corroborating data from genome sequence analysis (18, 25, 26).

The labeling profiles reflected only minor flux from pyruvate to oxaloacetate as well as from oxaloacetate to phosphoenolpyruvate/pyruvate by reactions of gluconeogenesis (including formation of [$^{13}C_2$]Ser indicating that Ser can be made *de novo*). This is surprising because it was believed that the EMP pathway is used in the direction of gluconeogenesis and that Ser or pyruvate is required to maintain a pool of oxaloacetate (high activity of pyruvate carboxylase (20)). In addition, our results could not corroborate minor flux from pyruvate to acetyl-CoA, as suggested earlier on the basis of low activity for pyruvate dehydrogenase in cell lysates of *Lp* (20). However, at this time it is not possible to reach a conclusion on the importance of gluconeogenesis for *Lp*. Experiments are under way to investigate this question further.

The fact that many amino acids (Leu, Ile, Val, Phe, Tyr, Met, Arg, and His) were unlabeled corroborate that *Lp* is auxotrophic for many amino acids, as suggested by genome analysis (16, 18), and that amino acids (including Ser) can act as major carbon substrates for *Lp*. On the other hand, the detection of diluted label from exogenous [U-$^{13}C_3$]Ser in metabolites derived from downstream central intermediates (*i.e.* acetyl-CoA, oxaloacetate, and α-ketoglutarate) lends support for the use of additional non-amino acid carbon substrates.

Inspired by this observation, we performed labeling experiments with 11 mm [U-$^{13}C_6$]- or [1,2-$^{13}C_2$]glucose as a supplement to AYE medium or CDM. In both experimental settings, glucose was incorporated into amino acids and PHB, affording ^{13}C enrichments up to 10% in pyruvate/Ala. Again, minor amounts of Ser were synthesized *de novo* in this experiment. Generally, the transfer of label from glucose to central metabolic intermediates providing precursors of the labeled amino acid is surprising, because it is believed that glucose or carbohydrates are not utilized by *Lp* (12, 15, 18, 20). Although the glycolytic pathway appeared to be complete (as suggested from the sequenced genomes), enzymatic assays indicated very low, if any, metabolic flux through this route (14, 16, 20). In addition, we confirmed that *Lp* does not exhibit a functional PP pathway, corroborated by the lack of orthologues of 6-phosphogluconate dehydrogenase and transaldolase within the recently sequenced *Lp* genomes. The ED pathway was also not thought to be active (16, 18). However, in our

experiments, the labeling profiles of PHB and amino acids demonstrated carbon flux from glucose to pyruvate via the ED pathway and not via the EMP and/or the PP pathway. As further strong evidence, the Δ*zwf* mutant of *Lp* Paris, impaired in the key reaction of the ED pathway, was strongly reduced in its glucose utilization. However, the deletion of the *zwf* gene would also affect the catabolism of glucose via the PP pathway; but this seems to be a negligible concern, because our results (WT strain) demonstrated that the PP pathway was not used for glucose catabolism by *Lp*.

Further analysis of the putative *zwf* operon demonstrated that the genes *lpp0483* to *lpp0487* are transcribed as one mRNA unit. The putative glucose transport protein encoding gene *lpp0488* is transcribed separately as a monocistronic mRNA. It is also noteworthy that the glucokinase (*glk*, *lpp0486*) is located within the *zwf* operon encoding for genes of the ED pathway. The products of glucose degradation by the encoded enzymes of the *zwf* operon would be glyceraldehyde 3-phosphate and pyruvate, which could then enter into the lower part of glycolysis and the citrate cycle, respectively (see Fig. 7).

Further analysis of the Δ*zwf* mutant strain demonstrated that the mutant strain was outcompeted by the wild type strain in a combined replication/survival assay with successive rounds of infection (Fig. 8*D*). In the first round of infection, the Δ*zwf* mutant strain replicated as well as the wild type strain; however, during repeated infection cycles, the fitness of the Δ*zwf* mutant strain was reduced in the presence of the wild type strain. Thus, the activity of glucose-6-phosphate dehydrogenase (ED pathway) and of glucose catabolism in general is important for full fitness of *Lp*.

In this context, it is important to note that *Lp* is also able to degrade cellulose (29), and we have identified a glucoamylase in *Lp* Paris the activity of which is responsible for starch and glycogen degradation of this strain.[6] Moreover, it has been shown that a mutation in the chitinase gene (*chiA*) has a negative effect on the virulence of the mutant strain as compared with the isogenic wild type strain (40). Preliminary labeling experiments of *A. castellanii*, the host organism, were successful. Thus we now have an excellent basis for *in vivo* infection experiments using *Lp* and "prelabeled" *A. castellanii* cells to analyze the intracellular metabolism of the human pathogen *Lp*. This will provide further information for better understanding the mechanisms of intracellular pathogens and how *Lp* gets access to essential nutrients during intracellular parasitism of amoebae.

In summary, we were able to demonstrate that (i) Ser is used efficiently as a carbon source but is also synthesized *de novo* by *Legionella*, although Ser is absolutely required for *in vitro* and *in vivo* growth of *Lp*; (ii) glucose is metabolized mainly via the ED pathway, which is active during *in vitro* growth, and not via the EMP or PP pathway; (iii) carbon from glucose is incorporated preferably into the storage compound PHB; (iv) the citrate cycle is complete and active; (v) *Lp* is not able to synthesize Ile, Leu, Val, Phe, Met, Arg, and Tyr; and (vi) glucose metabolism via the ED pathway is necessary for full fitness of *Lp* during its life cycle.

Acknowledgments

We thank Kerstin Rydzewski and Christine Schwarz for technical assistance.

References

1. Garduno, R. A., Gardun˜o, E., Hiltz, M., and Hoffman, P. S. (2002) *Infect. Immun.* 70, 6273–6283
2. Hammer, B. K., Tateda, E. S., and Swanson, M. S. (2002) *Mol. Microbiol.* 44, 107–118
3. Molofsky, A. B., and Swanson, M. S. (2003) *Mol. Microbiol.* 50, 445–461
4. Molofsky, A. B., and Swanson, M. S. (2004) *Mol. Microbiol.* 53, 29–40
5. Swanson, M. S., and Hammer, B. K. (2000) *Annu. Rev. Microbiol.* 54, 567–613
6. Greub, G., and Raoult, D. (2003) *Res. Microbiol.* 154, 619–621
7. Anderson, A. J., and Dawes, E. A. (1990) *Microbiol. Rev.* 54, 450–472
8. Anderson, A. J., Haywood, G. W., and Dawes, E. A. (1990) *Int. J. Biol. Macromol.* 12, 102–105
9. Steinert, M., Emödy, L., Amann, R., and Hacker, J. (1997) *Appl. Environ. Microbiol.* 63, 2047–2053
10. Pine, L., George, J. R., Reeves, M. W., and Harrell, W. K. (1979) *J. Clin. Microbiol.* 9, 615–626
11. Reeves, M. W., Pine, L., Hutner, S. H., George, J. R., and Harrell, W. K. (1981) *J. Clin. Microbiol.* 13, 688–695
12. Ristroph, J. D., Hedlund, K. W., and Gowda, S. (1981) *J. Clin. Microbiol.* 13, 115–119
13. Tesh, M. J., and Miller, R. D. (1982) *Can. J. Microbiol.* 28, 1055–1058
14. Tesh, M. J., Morse, S. A., and Miller, R. D. (1983) *J. Bacteriol.* 154, 1104–1109
15. Weiss, E., Peacock, M. G., and Williams, J. C. (1980) *Curr. Microbiol.* 4, 1–6
16. Fonseca, M. V., Sauer, J. D., and Swanson, M. S. (2008) in *Legionella-Molecular Microbiology* (Heuner, K., and Swanson, M. S., eds) pp. 213–226, Horizon Scientific Press, Norfolk, United Kingdom
17. Hoffman, P. S. (1984) in *Proceedings of the 2nd International Symposium on Legionella* (Thronsberry, C., Balows, A., Feeley, J. C., and Jakubowsky, W., eds) pp. 61–67, American Society for Microbiology, Washington, D. C.
18. Hoffman, P. S. (2008) in *Legionella pneumophila: Pathogenesis and Immunity* (Hoffman, P. S., Klein, T., and Friedman, H., eds) pp. 113–131,Springer Publishing Corp., New York
19. Wieland, H., Ullrich, S., Lang, F., and Neumeister, B. (2005) *Mol. Microbiol.* 55, 1528–1537
20. Keen, M. G., and Hoffman, M. S. (1984) *Curr. Microbiol.* 11, 81–88
21. George, J. R., Pine, L., Reeves, M. W., and Harrell, W. K. (1980) *J. Clin. Microbiol.* 11, 286–291
22. Ristroph, J. D., Hedlund, K. W., and Allen, R. G. (1980) *J. Clin. Microbiol.* 11, 19–21
23. Weiss, E., and Westfall, H. N. (1984) *Appl. Environ. Microbiol.* 48, 380-385
24. Tesh, M. J., and Miller, R. D. (1981) *J. Clin. Microbiol.* 13, 865–869
25. Cazalet, C., Rusniok, C., Brüggemann, H., Zidane, N., Magnier, A., Ma, L., Tichit, M., Jarraud, S., Bouchier, C., Vandenesch, F., Kunst, F., Etienne, J., Glaser, P., and Buchrieser, C. (2004) *Nat. Genet.* 36, 1165–1173
26. Chien, M., Morozova, I., Shi, S., Sheng, H., Chen, J., Gomez, S. M., Asamani, G., Hill, K., Nuara, J., Feder, M., Rineer, J., Greenberg, J. J., Steshenko, V., Park, S. H., Zhao, B., Teplitskaya, E., Edwards, J. R., Pampou, S., Georghiou, A., Chou, I. C., Iannuccilli, W., Ulz, M. E., Kim, D. H., Geringer-Sameth, A., Goldsberry, C., Morozov, P., Fischer, S. G., Segal, G., Qu, X., Rzhetsky, A., Zhang, P., Cayanis, E., De Jong, P. J., Ju, J., Kalachikov, S., Shuman, H. A., and Russo, J. J. (2004) *Science* 305, 1966–1968
27. Sauer, J. D., Bachman, M. A., and Swanson, M. S. (2005) *Proc. Natl. Acad. Sci. U.S.A.* 102, 9924–9929
28. Brüggemann, H., Hagman, A., Jules, M., Sismeiro, O., Dillies, M. A., Gouyette, C., Kunst, F., Steinert, M., Heuner, K., Coppée, J. Y., and Buchrieser, C. (2006) *Cell. Microbiol.* 8, 1228–1240
29. Pearce, M. M., and Cianciotto, N. P. (2009) *FEMS Microbiol. Lett.* 300, 256–264
30. Glöckner, G., Albert-Weissenberger, C., Weinmann, E., Jacobi, S., Schunder, E., Steinert, M., Hacker, J., and Heuner, K. (2008) *Int. J. Med. Microbiol.* 298, 411–428
31. Banerji, S., Aurass, P., and Flieger, A. (2008) *Int. J. Med. Microbiol.* 298, 169–181
32. Flieger, A., Rydzewski, K., Banerji, S., Broich, M., and Heuner, K. (2004) *Infect. Immun.* 72, 2648–2658
33. Schunder, E., Adam, P., Higa, F., Remer, K. A., Lorenz, U., Bender, J., Schulz, T., Flieger, A., Steinert, M., and Heuner, K. (2010) *Int. J. Med. Microbiol.* 300, 313–323
34. Zamboni, N., Fendt, S. M., Rühl, M., and Sauer, U. (2009) *Nat. Protoc.* 4, 878–892
35. Sauer, U., and Eikmanns, B. J. (2005) *FEMS Microbiol. Rev.* 29, 765–794
36. Eisenreich, W., Slaghuis, J., Laupitz, R., Bussemer, J., Stritzker, J., Schwarz, C., Schwarz, R., Dandekar, T., Goebel, W., and Bacher, A. (2006) *Proc. Natl. Acad. Sci. U.S.A.* 103, 2040–2045
37. Eylert, E., Schär, J., Mertins, S., Stoll, R., Bacher, A., Goebel, W., and Eisenreich, W. (2008) *Mol. Microbiol.* 69, 1008–1017

38. Heuner, K., Dietrich, C., Skriwan, C., Steinert, M., and Hacker, J. (2002) *Infect. Immun.* 70, 1604–1608
39. Lee, W. N., Byerley, L. O., Bergner, E. A., and Edmond, J. (1991) *Biol. Mass Spectrom.* 20, 451–458
40. DebRoy, S., Dao, J., Söderberg, M., Rossier, O., and Cianciotto, N. P. (2006) *Proc. Natl. Acad. Sci. U.S.A.* 103, 19146–19151

Tables and Figures

Table 1 Primers used in this study

Oligonucleotide	Sequence
PCR	
lpp0483_for	TACATTGAGAAAAAAGCGAAGCCAA
lpp0483_rev	TGCTGTTTAATAATCGCCTTTTCGA
lpp0483_inv_for	ACAGCCTTATAATATCTTTC
lpp0483_inv_BamHI_rev	CGGGATCCCGGTTAATTTTTGATAATCATC
Kan_BamHI_for	CGGGATCCCGCTATCTGGACAAGGGAAAAC
Kan_BamHI_rev	CGGGATCCCGGAAGAACTCCAGCATGAGAT
RT-PCR	
accC-For	GAACTTGGCATTCAGACTGTTGC
accC-Rev	AGCATGTCCTTTCCCATCACC
edd-For	AGAGCAGCTTATCTGAATCAAATGG
edd-Rev	AAAACCTGCAAACCACCCTGA
fadD-For	AATGGAGTACCACATGAAATTGACG
fadD-Rev	CCAGAGGAGATATCCAGGTGTA
fumC-For	AACACGTGTAGAAACAGACAGCATG
fumC-Rev	AGGGGTTCATGAGAAGCCAGA
pfp-For	CTGGTGGTGTGACCGCTGTAA
pfp-Rev	GGGACTTGGCCTATAGACCATT
pgl-edd-For	CTAGAACAGCTTCATTCCAGAG
pgl-edd-Rev	GAGTACGGTTGATGCGCTTATA
pykA-For	GCCAGTAAGGAACCTGAAATTCTG
pykA-Rev	CTTCTGCTTCAATTGCTGTACGC
ppsA-For	ACTATAGATTTGGCACATCTTGGCA
ppsA-Rev	GGGTTTCCAACATTCAACATCACT
rpiA-For	AAGAACTGGCAGCAATCAAACAC
rpiA-Rev	CCAAGGCCATAGGTGTTGAGAA
sucA-For	TTGTCTGGAGGAAGTATGGCTTATG
sucA-Rev	TGAAGGGTTAAACGCCAAAGC
zwf-pgl-For	GCCAAAGGAAGTCATACGCTTA
zwf-pgl-Rev	GAGAATCAATTTGGCTATTCACC

Table 2 NMR data of ^{13}C-labeled PHB obtained from incorporation experiments with *Lp*

Carbon	Chemical shift	$^{13}C^{13}C$ coupling constant[a]
	ppm	*Hz*
1	169.10	58.1 (2)
2	40.75	58.1 (1); 39.5 (3)
3	67.55	39.4 (2); 39.0 (4)
4	19.72	38.9 (3)

[a] Coupling partners are indicated in parentheses.

Figure 1 Formation of PHB in experiments with [U-$^{13}C_3$]Ser and [U-$^{13}C_6$]glucose. Multiple ^{13}C labeling is indicated by *bars* connecting ^{13}C-labeled atoms. The patterns of acetoacetyl-CoA and downstream products are overlays of isotopologues comprising two ^{13}C-labeled atoms in a single molecule.

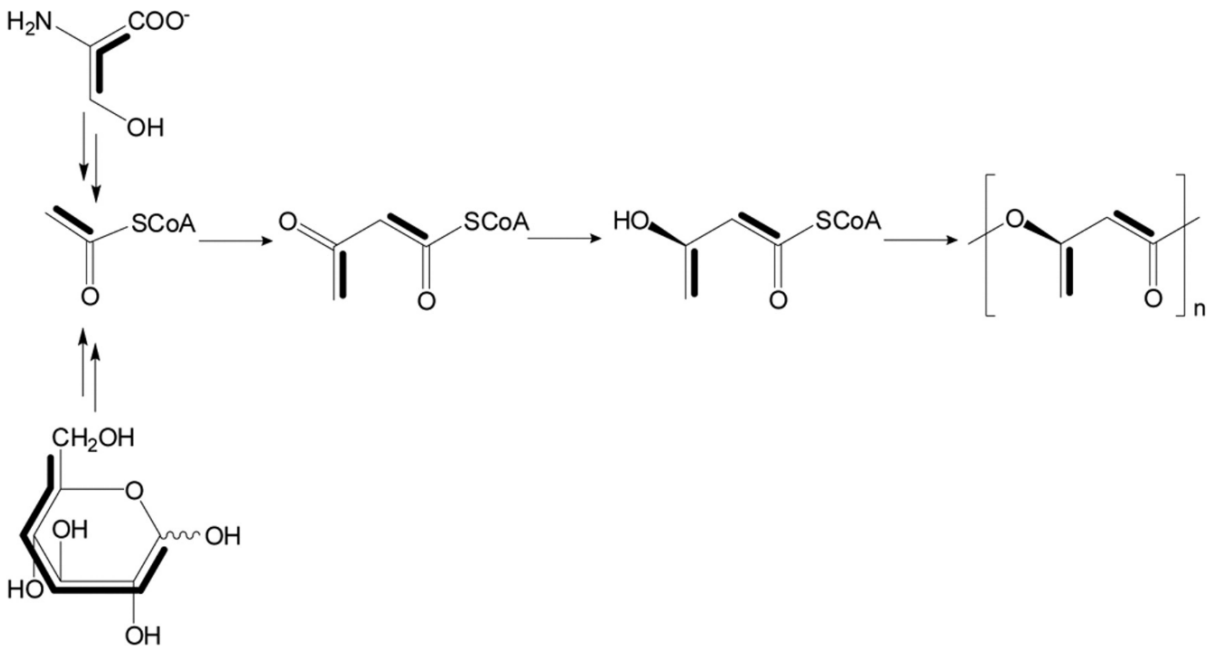

Figure 2. ^{13}C excess (*gray columns*; in mol % (*right scale*)) and isotopologue composition (*patterned columns*) of amino acids from the experiment with [U-$^{13}C_3$]Ser. The values represent means from three technical replicates, and the *error bars* indicate S.D. The *patterned boxes* indicate the relative contribution (% (*left scale*)) of ^{13}C-isotopologues (M+1 to M+5 in different patterns) in the overall enrichments.

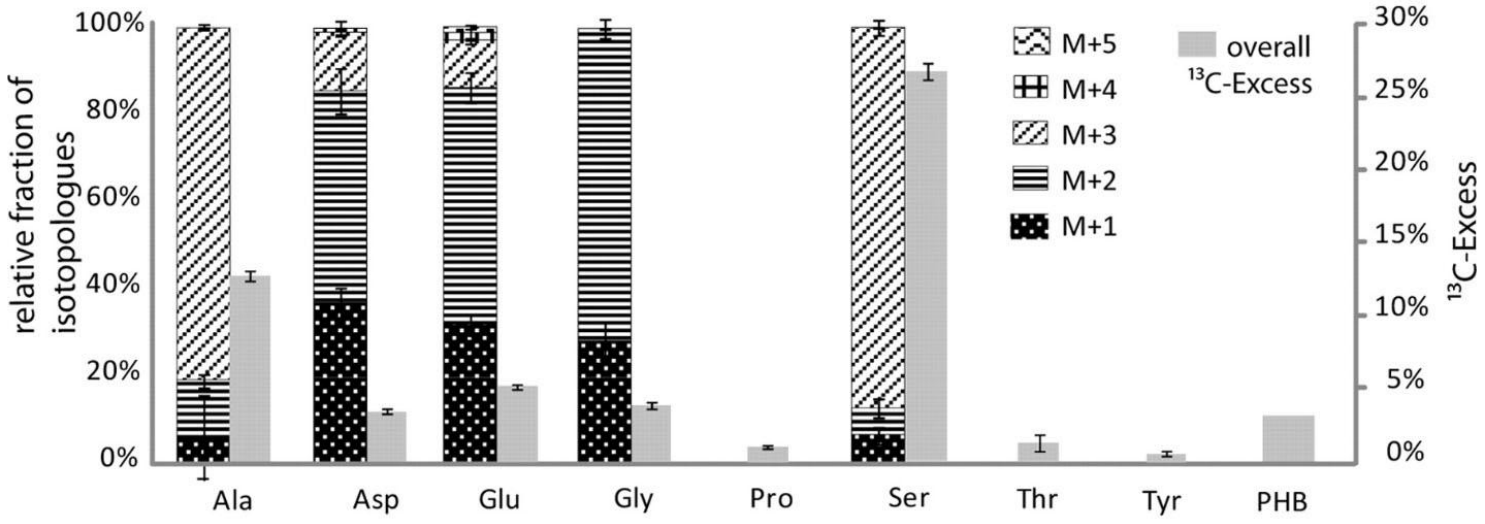

Figure 3 Metabolic model for Ser utilization by *Lp* Paris grown in culture. The scheme shows labeling patterns due to the incorporation of exogenous [U-$^{13}C_3$]Ser. Labeling patterns were detected in protein-derived amino acids and PHB (shown in *boxes*). Multiple ^{13}C-labeled isotopologues determined by NMR spectroscopy are indicated as *bars* connecting ^{13}C-labeled atoms in a given molecule. The *numbers* indicate the respective molar abundances. The molar abundances of isotopomer groups comprising one, two, or three ^{13}C-labeled atoms, as determined by mass spectrometry (M+1, M+2, and M+3, respectively), are also listed in the *boxes. PEP*, phosphoenolpyruvate; *OAA*, oxaloacetate; α-*KG*, α-ketoglutarate.

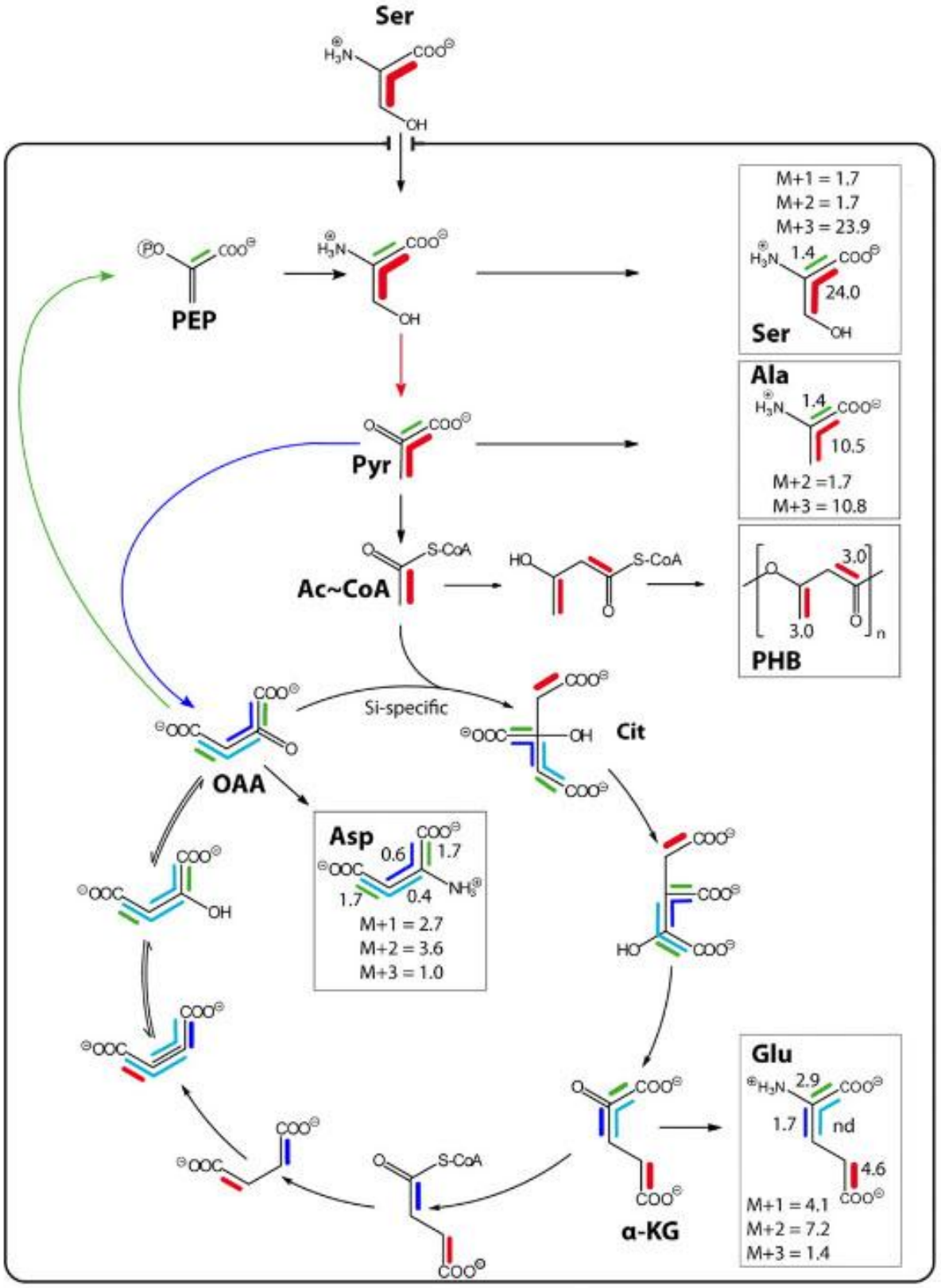

Figure 4 Overall ^{13}C excess (mol %) of labeled isotopologues in amino acids derived from protein after feeding of *L. pneumophila* Paris wild type and Δ*zwf* mutant with 11 mm [U-$^{13}C_6$]glucose and 11 mm [1,2-$^{13}C_2$]glucose in different media. The *color map* indicates ^{13}C excess in quasi-logarithmic form to show even relatively small ^{13}C excess values. Each sample (different labeling experiments) was measured three times; the *color* for each amino acid correlates with the mean value of the three measurements. *Asterisks* indicate S.D. > 35%. PHB could not be measured in the experiment with [1,2-$^{13}C_2$]glucose and the Δ*zwf* mutant.

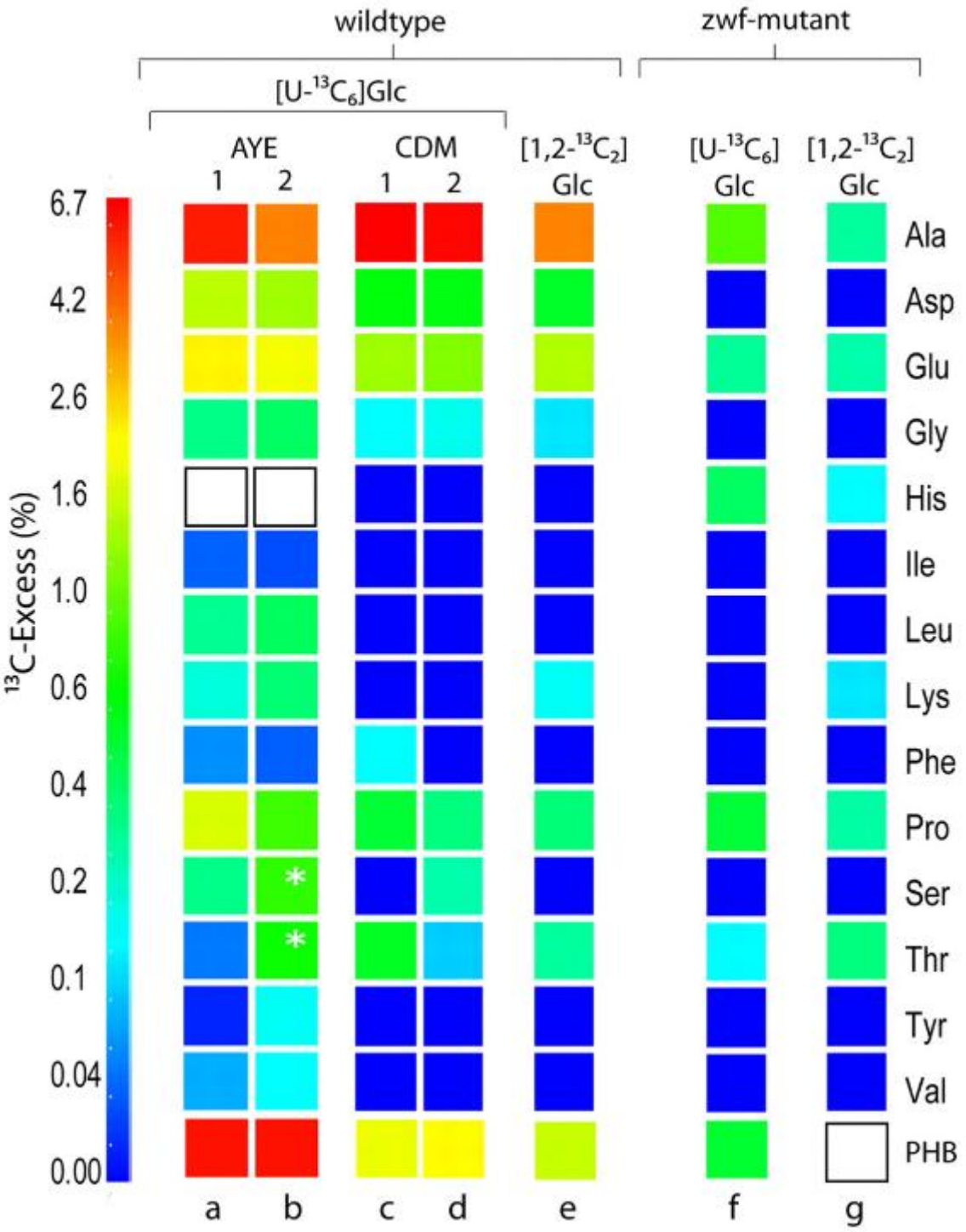

Figure 5. ^{13}C excess (*gray columns*; in mol % (*right scale*)) and isotopologue composition (*patterned columns*) of amino acids from experiments *1* and *2* with *L. pneumophila* wild type cultivated in AYE medium containing 11 mm [U-$^{13}C_6$]glucose. The values represent means from three measurements, and *error bars* indicate S.D. The *patterned boxes* indicate the relative contribution (% (*left scale*)) of ^{13}C-isotopologues (M+1 to M+5) in the overall enrichments.

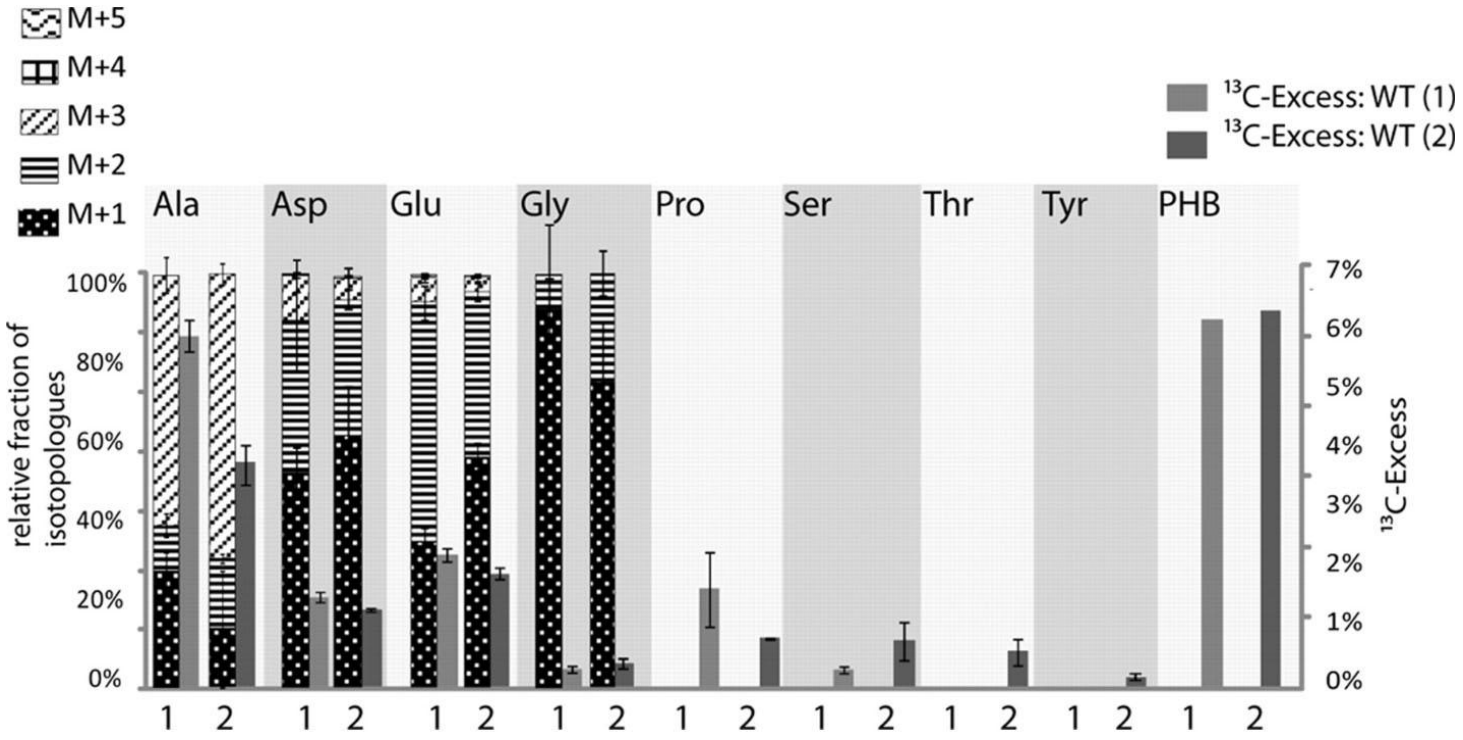

Figure 6. Metabolic model for glucose utilization in *Lp* Paris grown in AYE medium supplemented with [U-$^{13}C_6$]glucose. Labeling patterns were detected in protein-derived amino acids and PHB (shown in *boxes*). Multiple ^{13}C-labeled isotopologues determined by NMR spectroscopy are indicated as *bars* connecting ^{13}C-labeled atoms in a given molecule. The *numbers* indicate the respective molar abundances. The molar abundances of isotopomer groups comprising one, two, or three ^{13}C-labeled atoms as determined by mass spectrometry (M+1, M+2, and M+3, respectively) are also listed for comparison. *GAP*, glyceraldehyde-3-phosphate dehydrogenase; *6-P-Glcn*, 6-phosphogluconate; *Pyr*, pyruvate; *OAA*, oxaloacetate; α-*KG*, α-ketoglutarate.

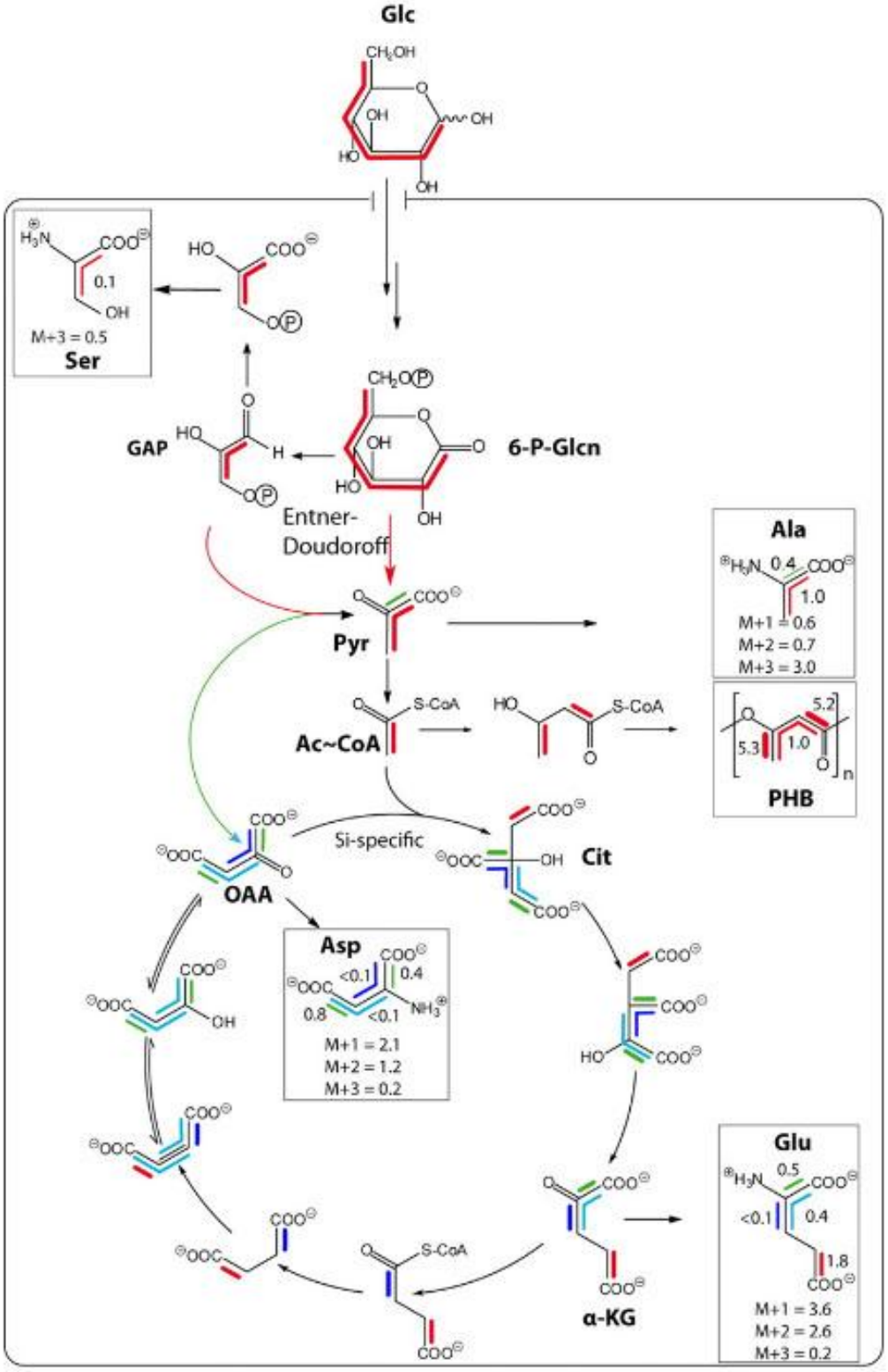

Figure 7. *A*, proposed EMP, ED, and PP pathways. The names of putative enzymes are shown; beneath them are the encoding open reading frames of Lp Paris (*lpp*), and the FC value of microarray analysis *in vitro* (28) are given in parentheses. *FC*, fold-change values (exponential phase versus stationary phase). Enzymes marked with an *asterisk* have no annotated homologues in the *Lp* genome. Genes determined to be co-transcribed are highlighted in *gray* and *dark gray*, respectively. *Glk*, glucokinase; *Pgi*, phosphoglucose isomerase; *Pfk*, phosphofructokinase; *Fba*, fructose-bisphosphate aldolase; *TpiA*, triose-phosphate isomerase; *Gap*, glyceraldehyde-3-phosphate dehydrogenase; *Pgk*, phosphoglycerate kinase; *Pgm*, phosphoglycerate mutase; *Eno*, enolase; *PykA*, pyruvate kinase; *Zwf*, glucose-6-phosphate dehydrogenase; *Pgl*, phosphogluconolactonase; *Edd*, phosphogluconate dehydratase; *Eda*, 2-keto-3-deoxy-phosphogluconate aldolase; *Gnd*, 6-phosphogluconate dehydrogenase; *Rpe*, ribulose phosphate-3-epimerase; *RpiA*, ribose-5-phosphate isomerase; *TktA*, transketolase; *Tal*, transaldolase; *Gcd*, glucose dehydrogenase; *Gnt*, gluconate transporter (modified from Ref. 16). *B*, schematic overview of the genes *lpp043–lpp0488* (*right*) and *lpp0150–lpp0154* (*left*). mRNA transcripts were determined via RT-PCR. *lpp0483*, *zwf*, *lpp0484*, *pgl*; *lpp0485*, *edd*; *lpp0486*, *glk*; *lpp0487*, *eda*; *lpp0488* (putative sugar transport protein); *lpp0150*, *sdhB* (substrate of the Dot/Icm system); *lpp0151*, *pykA*; *lpp0152*, *pgk*; *lpp0153*, *gap*; *lpp0154, tktA*.

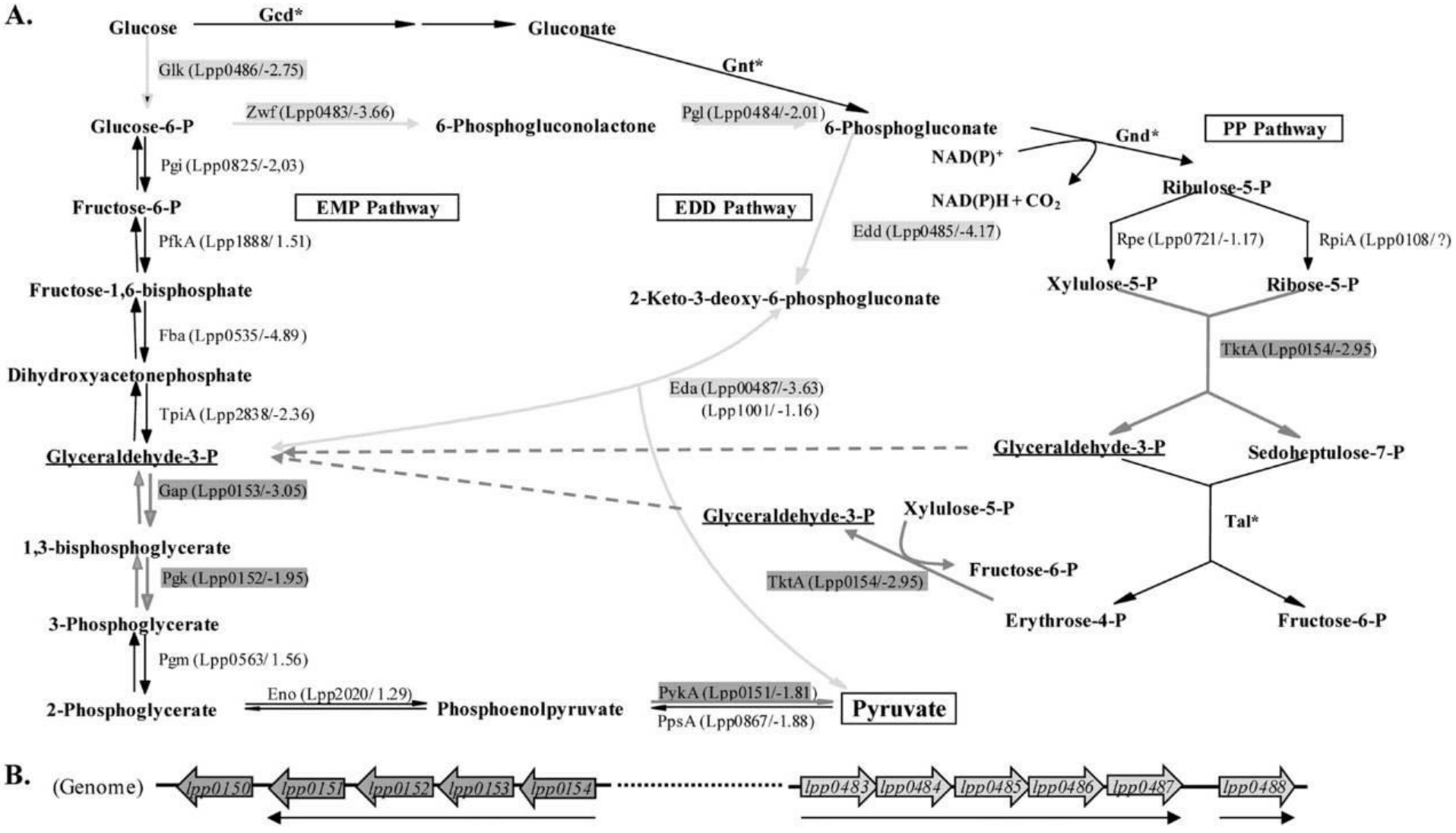

Figure 8. Analysis of *L. pneumophila* Paris (*WT*) and Δ*zwf* mutant strain (*zwf*−) in co-cultures with *A. castellanii*. Bacteria were used to infect monolayers of *A. castellanii* at a multiplicity of infection of 0.01 with (*A*) *Lp* Paris or the Δ*zwf* mutant strain for 96 h (*A*); *Lp* Paris or Δ*zwf* mutant strain for 3 days, resuspended and incubated for a further 3 days, diluted to ~10^3 bacteria/ml, and used to infect fresh amoebae (*B*). Four rounds of infection were performed. *C*, *L. pneumophila* Δ*zwf* and WT strain survival over a 20-day period after co-infection of *A. castellanii* cells at two different ratios (*circles*, 50:50; *diamonds*, 75:25). *D*, infection was done as described in *B*, but *A. castellanii* cells were infected with both strains (WT and Δ*zwf*) at the same time (in competition). At various time points postinoculation, bacteria were quantitated by plating aliquots on BCYE agar (see "Experimental Procedures"). Results are means ± S.D. of duplicate samples and are representative of at least three independent experiments.